Human Biomics Lab

Paulo Coelho
Timothy G. Bromage

Challenges in engineering and testing of bioceramics

High-Strength ceramics: Interdisziplinary perspectives

Chapter 1

The Challenges in Engineering and Testing Dental Bioceramics

by

Paulo Coelho and Timothy G. Bromage

Introduction

The clinical success of modern dental ceramics is predicated on a number of factors, such as the initial physical properties of these brittle materials, the fabrication and clinical procedures that unavoidably damage them, and the oral environment. Examining how these factors influence clinical performance has involved investigators from the dental, ceramics, and engineering communities. This chapter will first summarize the rationale behind engineering biomimetic ceramic dental restorative materials, then critically describe the basic methodology and analytic results reported in recent literature.

Basic Properties of Enamel and Dentin as Objectives for Bioceramic Development

There are several important properties of tooth structure relevant to bioceramic biomimetic design. Paramount is (1) *mechanical efficacy,* largely a function of tooth crown morphology, enamel thickness and microstructure, and root structure. Related to this is (2) *proprioception,* the internal perceptions that allow us to reduce the probability of catastrophic fracture from excessive loads transmitted through enamel into dentine and the supporting structures. An additional consideration is (3) the *porosity* of healthy enamel. Further, it is fair to say that people who take their oral care seriously enough to be receiving bioceramic implants will also be concerned with (4) the *aesthetics* of their natural teeth. Finally, if properly managed, enamel surfaces will support (5) a *biofilm* characteristic of healthy oral flora.

Mechanical Efficacy

Before considering enamel mechanical efficiency, a bit of background is necessary. Secretory ameloblasts secrete proteins responsible for the nucleation, regulation, and growth of enamel crystallites. During early stages of amelogenesis, enamel contains a high proportion of protein, which is soon rapidly removed by the enzymatic activities of these same cells, eliminating the vast proportion of protein and facilitating further growth in diameter of long and slender crystallites. Enamel ultimately reaches roughly 95% by weight carbonated hydroxylapatite $Ca_{10}(PO_4)_6(OH)_2$ (otherwise known as hydroxyapatite), 3–4% protein, and 1–2%

water—a composition yielding enamel's unique mechanical properties, which enable it to last the lifetime of most individuals. Reviews of the molecular, cellular, and physicochemical processes concerning enamel matrix formation, ion transport, and regulation of extracellular pH are available in the literature (1, 2).

The mechanical efficacy of a tooth—a natural functionally graded material—is a function of hierarchy of scale and material properties. Macroscopically, the mechanical loading and maximum stress distribution experienced by a tooth and its surrounding structures depend upon the incursive, intercuspal, and excursive contacts that characterize an individual's masticatory function (3). A load transmitted through the enamel and coronal dentine, the root(s), and periodontal ligament to the surrounding bone, when examined by finite element analysis of the deformation of the jaw, reveals how stress and strain vary as a result of highly specific occlusal collisions (4). Thus, an evaluation of opposing contact facets must remain among the highest of priorities for customized bioceramic tooth design if an individual's functional balance is to be achieved and maintained.

At a level down the hierarchy of scale is enamel thickness. Human first molar maximum cuspal thicknesses are about 2 mm (5). Among primates, humans are deemed to have thick enamel, it being considerably thicker than, say, that of a gorilla or chimpanzee. Our thick enamel reveals the evolutionary legacy of modern humans, which included a diet of hard and tough food items (6) whose mechanical properties far exceed those of foods eaten by industrialized people today. The substance of enamel, harboring, as it does, compositional and microstructural characteristics that inhibit the initiation and propagation of cracks (see below), makes thick enamel an important geometric property bearing on masticatory mechanics.

Through the substance of human enamel and the immediately underlying dentine there exist compositional variations regarded as "graded structures." Material density transitions (i.e., of mineralization) that are spatially sharp potentially engender differential strain either side of the border between phases, and such transitions are prone to fracture and separation upon physical or thermal stress. Human molar enamel reveals an astonishing gradation in both hardness and elastic modulus, diminishing from outer surface enamel toward the enamel–dentine junction (EDJ) (7). For instance, as stress reaches the EDJ the enamel becomes more compliant. The EDJ is also graded on the dentine side, being comparatively hard and stiff nearest the EDJ, with values like those of the adjacent enamel, then becoming gradually softer and yielding by some several hundred microns away from the EDJ (8-10).

A remarkable feature of mammalian enamel, particularly of those species whose diet comprises hard and tough food items, is a developmental pattern referred to as *enamel*

decussation, in which enamel prisms, or rods, cross paths at some angle and are visible as Hunter–Schreger bands by light microscopy (11) (Fig. 1). Secretory ameloblasts displace themselves outward from the EDJ in a direction opposite to the secretory face of their Tomes' process (Fig. 2). A group of, say, 10 cells thick takes a gently sinusoidal course outward at some angle (ca. 45°–55° depending upon species) to an adjacent group of cells (12). In modern human teeth, Hunter–Schreger bands are always present in the inner enamel, sometimes reaching the outer enamel, but sometimes dissipating before reaching the surface (11) (Fig. 3a–d). Importantly, the discontinuity of prism orientation that exists between groups of prisms functions to resist crack propagation (13). Because occlusal loads transmit through a stiff outer shell of enamel onto a relatively compliant landscape of dentine, peak tension is generated in the lowermost enamel as it tends to push inward at the EDJ. This establishes the presence of Hunter–Schreger bands, particularly at inner enamel locations, as an anti-crack-propagating adaptation in humans and other species (14, 15).
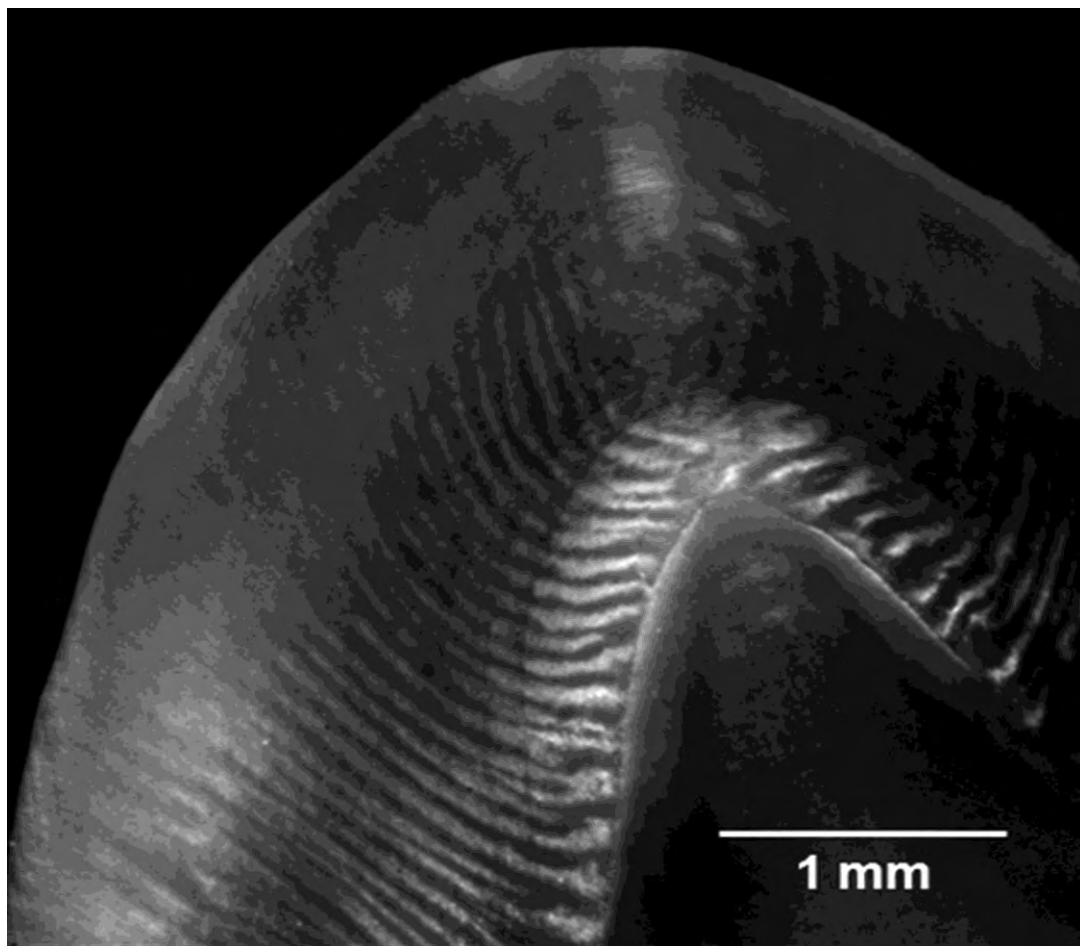

Figure 1. Linearly polarized reflected light image of human first molar mesiobuccal cuspal enamel cut in longitudinal section, obtained using a Leica MZ-APO stereo zoom microscope (Wetzlar, Germany). Hunter–Schreger bands (HSB) appear as alternating light and dark bands

that relate to enamel prisms occurring, respectively, in and out of the plane of section. HSB course from the enamel–dentin junction outward, dissipating toward the outer surface enamel.
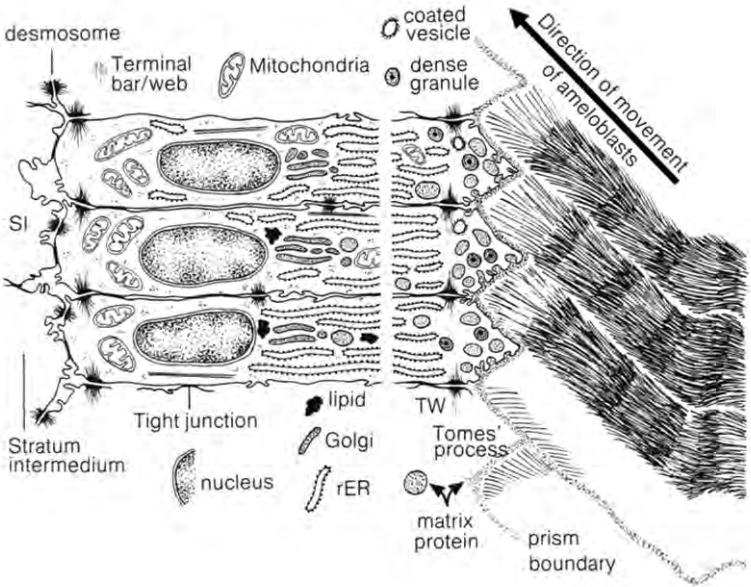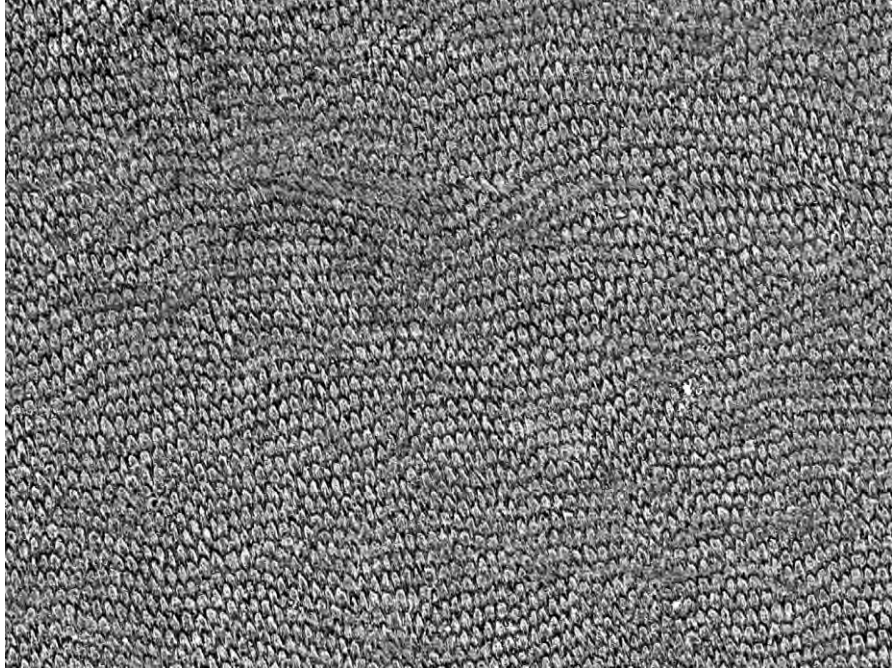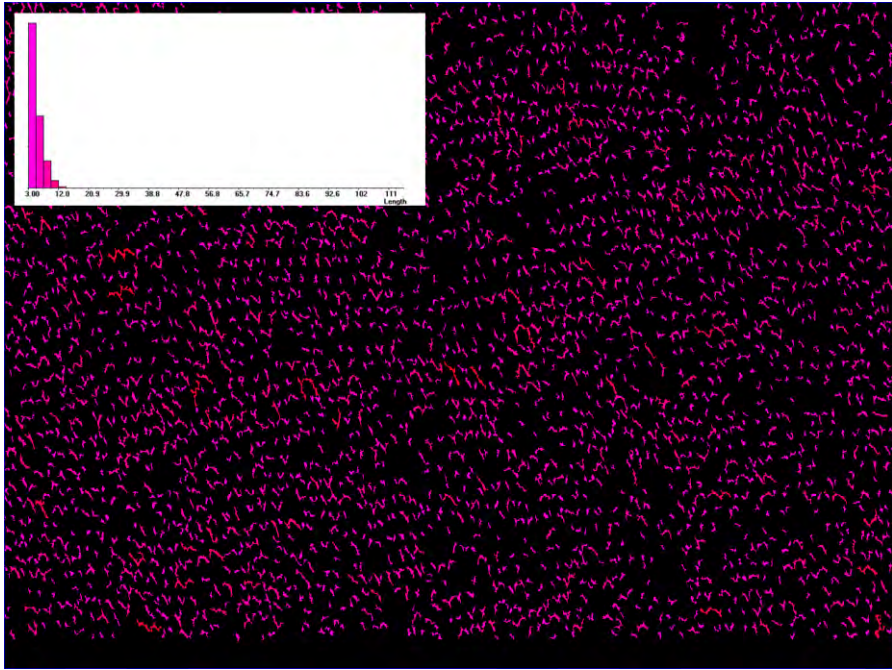

Figure 2. Diagram of the ameloblast (taken from Boyde 1989) (16). Note the asymmetry in matrix protein secretion and crystallite mineralization characteristic of human enamel formation.
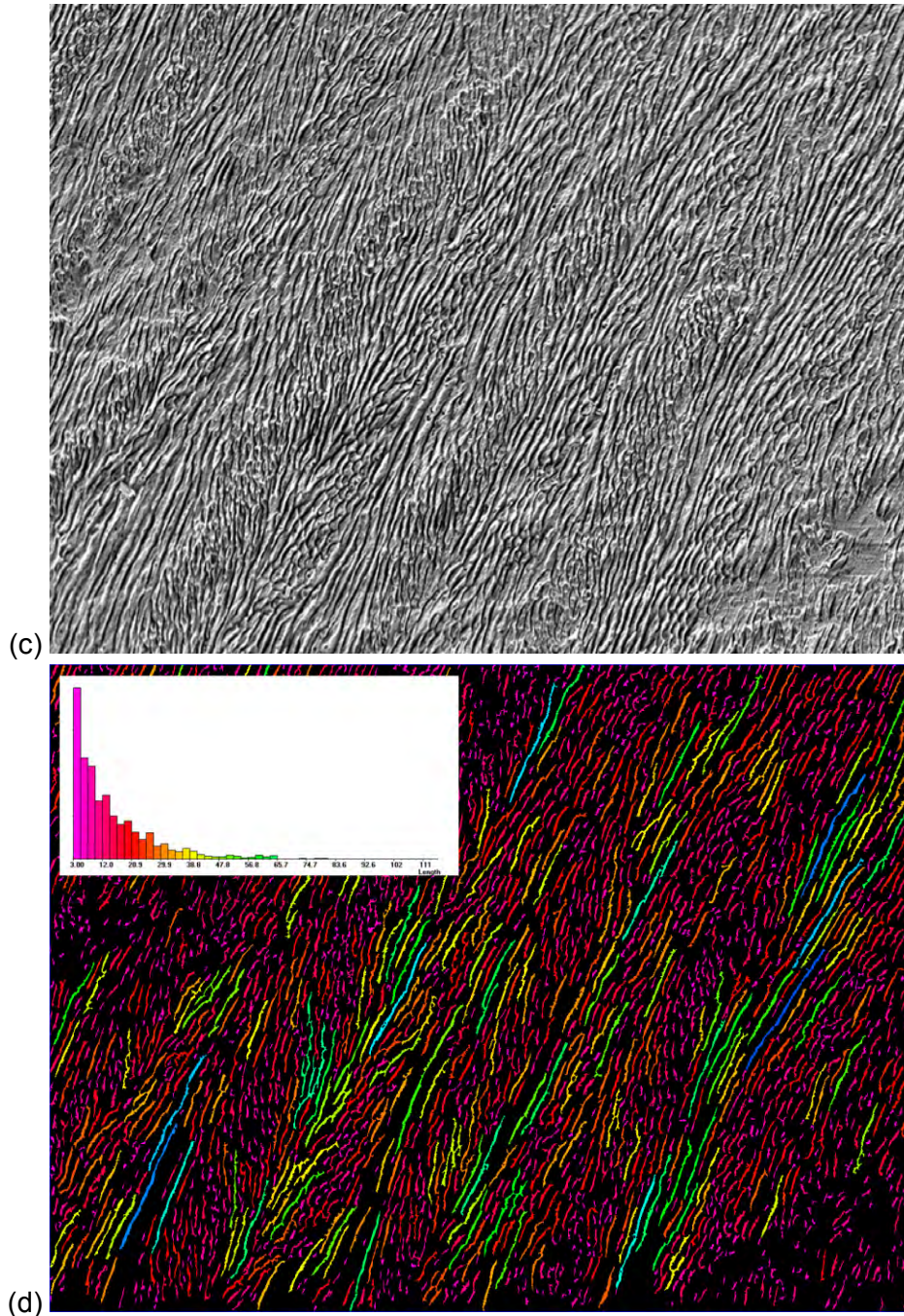
(a)

(b)

Figure 3. (a) Image of etched human mesiobuccal enamel in cross section 100 μm deep to the outer surface enamel, obtained using a backscattered electron detector in the Zeiss EVO 50 (Thornwood, NY) scanning electron microscope (BSE-SEM; uncoated at 15 kV, 600 pA current, 50 Pa pressure). (b) The BSE-SEM image in Fig. 3a was subjected to image analysis (Leica QWin 550 software) for measuring and color coding enamel prism aspect ratios (*inset:* aspect ratio distribution). (c) BSE-SEM image of human mesiobuccal enamel in cross section 800 μm deep to the outer surface enamel. (d) The BSE-SEM image in Fig. 3c also was subjected to image analysis for measuring and color coding enamel prism aspect ratios. Note the increase in enamel decussation (and aspect ratios) in mid-cuspal enamel. Field widths = 500 μm.

Enamel is also rich with additional discontinuities at the micron and nanometer scale (16, 17), complexities of which require some detailed explanation. Human enamel prisms are approximately the size of an ameloblast, roughly 5 μm in diameter (Fig. 4). They are characterized by a specific packing of crystallites, roughly 20–40 nm in diameter (Fig. 5), formed off of protein scaffolds synthesized from two locations. The first location is immediately below the junctional complexes (see Fig. 2), which ties the cells together and isolates their distal ends to a secretory compartment. This semicircular periphery forms a rim that, by its height difference, defines an inner pit. This so-called *interpit enamel* is formed of crystallites whose crystallographic *c*-axes run parallel with the prism orientation and effectively constitute a continuous phase from the EDJ to the outer surface enamel (Fig. 6). The open end of this collar of enamel is oriented in the cervical direction. The second location is the secretory pole of the cell, called the Tomes' process, which has an asymmetry, becoming flush with the interpit enamel on its cervical surface (i.e., open end of the collar). Matrix secretions from only that portion of the Tomes' process facing the developing enamel surface form the floor of the pit and its gently sloping surface leading up to the top of the floor and abutting interpit enamel formed by cells immediately cervical to it. Because enamel crystallographic *c*-axes orient perpendicular to the Tomes' process surface, variable crystallite orientations exist within the pit, being parallel with the prism at its coronally located back wall, becoming cervically rotated through roughly 45° at its junction with the interpit enamel formed by cells cervical to it (Fig. 6). This complex arrangement renders enamel crystallite discontinuities, represented by acute abutments between crystallites of different orientation, along which nanoscopic cracks may form, potentially generating sliding planes. Enamel crystallite discontinuities occur both between interpit and pit enamel arising from the same cell, and between the pit enamel of one cell and the interpit enamel formed by cervically adjacent cells.
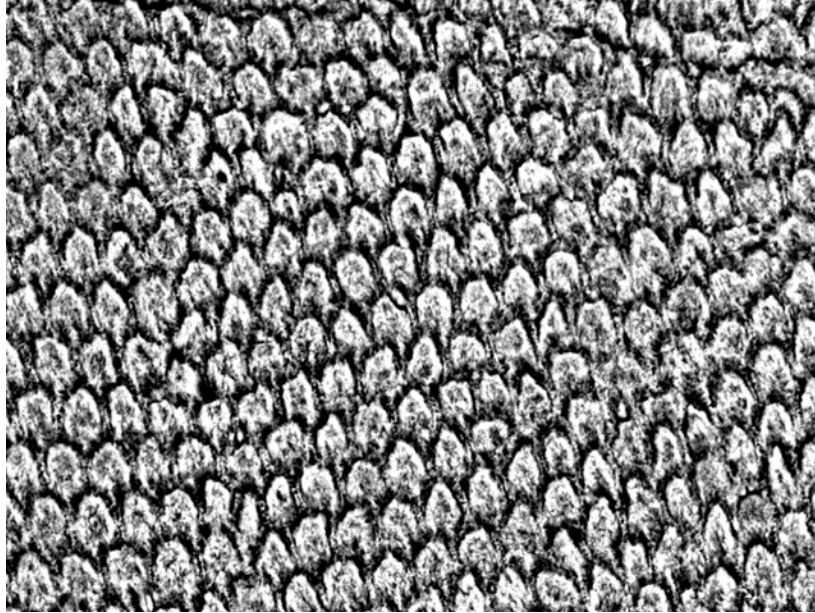
Figure 4. Image of etched human superficial mesiobuccal cuspal enamel obtained using a backscattered electron detector in the Zeiss EVO 50 scanning electron microscope (uncoated at 15 kV, 600 pA current, 50 Pa pressure). Brightness relates to mineralization density; brighter regions are more densely mineralized. Field width = 150 μm.
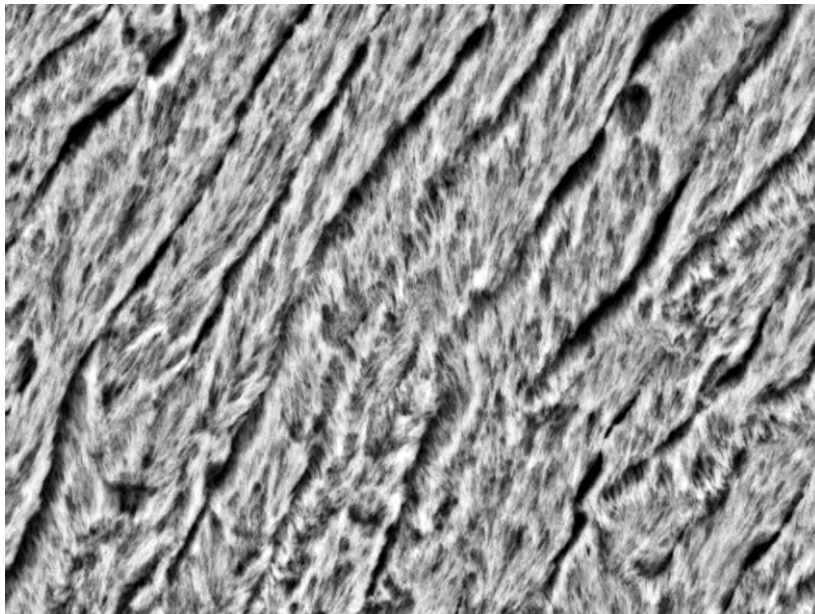

Figure 5. Image of needlelike enamel crystallites along etched enamel prisms (the fine fibrillar fabric in this image) using a backscattered electron detector in the Zeiss EVO 50 scanning electron microscope (uncoated at 15 kV, 100 pA current, 30 Pa pressure). Field width = 50 μm.
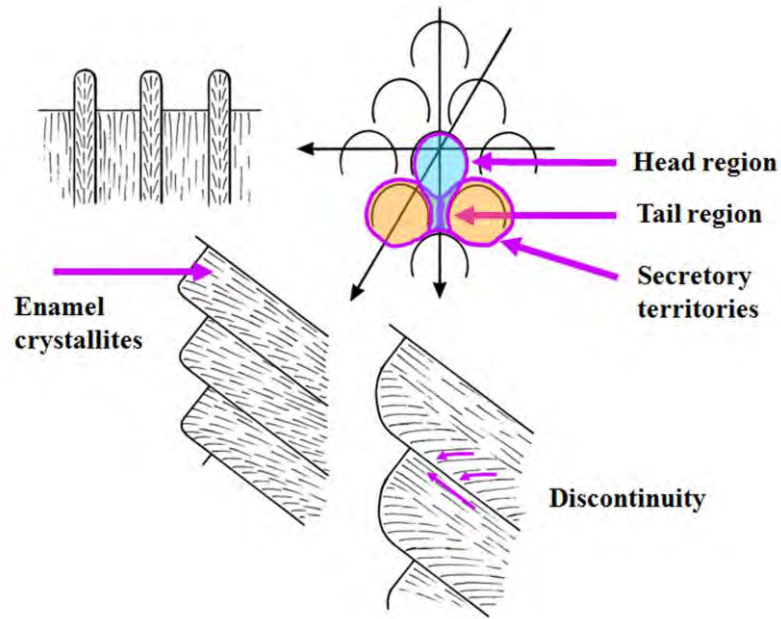
Figure 6. Diagrammatic cross section of human enamel prisms reveal a confluence of crystallites packed into the shape of a rounded head region (rod) and, directly cervical to this, its interrod enamel (tail). This structure has been likened to a "keyhole." Depending upon the section plane (black arrows, which point toward representations of crystallite orientations), a variety of enamel crystallite discontinuities can be observed. Figure adapted (from Boyde 1989)(16).

Since tooth structural formation takes place in such a complex and organized fashion, it is expected that subtle variations in ameloblast secretory rate and mineralization chemistry also occur over daily and near-weekly time frames in human enamel, producing incremental lines in enamel (16, 18). This compositional variability combines with subtle changes in crystallite orientation to produce another order of discontinuity. In addition, mineralization density differences—low mineral density in interpit enamel and the central region of pit enamel, relatively higher mineralization density in the peripheral pit floor—generate another discontinuity (see Fig. 4).

Nanoscopic fractures will always prefer paths of least resistance and follow the discontinuities mentioned above (19). Because of their heterogeneity, and because of the abutments created by discontinuities, such cracks tend to be arrested. These microdiscontinuities, combined with the macrodiscontinuity of decussating enamel, have the effect of situating crack-arresting abutments in all 360° spherical rotations, making enamel a supremely competent material under biological loading stress.

Since enamel crystallites are hexagonal in cross section, their flat faces have the potential to slip at nanometer and subnanometer scales, without fracture. This permits a small degree of strain in bulk enamel under load. This load is taken up mostly by crystallites, but as in many natural materials, is transferred to protein-laced shear zones between crystals (20), which absorb stress (21) and generate tethering ligaments between separating crystals (22). Such nanoscopic cracks that do emerge arrest at small length scales, effectively toughening the material.

A brief mention of the importance of water in hard tissues is warranted. Very little research into the presence and location of mobile and bound (i.e., structural) water in bone and tooth materials has been undertaken. Research on enamel is scarce, but the presence of bound water, presumably located within crystallite structure, and of mobile water are documented (23, 24). That mobile and bound water in bone have been shown to relate both to the modulus and strength of the tissue, respectively, is evidence of water's critical role in maintaining enamel mechanical integrity (25). Indeed, evidence from studies of nanoindentation creep in enamel demonstrates that dehydrated enamel has a significantly lower energy absorption than does sound enamel (21). Although water represents only 1–2% by weight of enamel, it has a profound influence on mechanical efficacy.

Finally, the wear characteristics of human enamel should be mentioned. Prism orientation is important both in relation to resistance to load (26) and to functional wear resistance (27). There is a fascinating diversity in prism orientation among mammals, some of which is designed to generate differential wear; but among humans, prisms (and their contained crystallites) arrive at rather steep angles to wear facets, providing excellent wear resistance (17, 28). This adaptation is clearly only one of a number of solutions taken by members of the human family (29), one that depends upon the dietary characteristics pertinent to niches occupied by early human species.

From an engineering materials and narrow mechanical efficiency perspective, bioceramic biomimetic designs are an ultimate challenge and would ideally include engineering materials that are three-dimensionally functionally graded at multiple length scales. In essence, enamel and dentine are hierarchically complex, with functionally graded structures of one length scale within functionally graded structures of another length scale, these having been finely tuned over millions of years of evolution. Current technologies enable a partial assembly of multiscale functionally graded structures. When materials assembly is possible at multiple length scales in three dimensions, the addition of components that will mimic the structural role of enamel's biologic components will be necessary if one is attempting to mimic enamel's

unique ability to hinder crack propagation. Finally, even if biomaterials scientists moving forward are able to design materials that mechanically function like enamel, proprioception, aesthetics, and other biocompatibility considerations are as important as the mechanical behavior of newly developed material.

Proprioception

Mechanoreceptors in some tendons and muscles of mastication, as well as in the periodontal ligament itself, provide feedback on jaw position and bite forces. Interruption to the normal rate and force applied during mastication may trigger an involuntary proprioceptive response. With respect to teeth, this is highly adaptive, allowing the masticatory system to recoil from accidentally applying an excessive and concentrated load capable of causing catastrophic fracture (e.g., as when biting down on a grain of sand). That receptors in the periodontal ligament are particularly important in this regard is suggested by the significantly blunted response of osteointegrated dental implants to occlusal forces (30). Thus, a bioceramic biomimetic design must either include some mechanism to provide natural feedback mechanisms to elicit avoidance of occlusion at unnaturally high forces, or else the materials used must include safety factors well beyond those of natural teeth.

Porosity

The mobile water in enamel passes through a system of small pores representing 6% by volume of the space thought to reside in the centers of prism heads, and larger pores representing 0.3% by volume at prism boundaries (31). Beyond the potential importance of this pore space and its contained water on the mechanical efficacy of enamel (as indicated above), the function of these spaces is also to participate in the diffusion of ions in and out of the tooth, such as has been reported for ^{45}Ca (32) and ^{32}P (33). That enamel has this permeability indicates that the constant and relatively rapid exchange of ions in and out of enamel is a normal process and one that has some adaptive value. Curiously, the nature of this adaptation has not received attention by enamel biologists, and we are left to speculate. Naturally, upsets of oral pH can perturb this process, and in the case of pH reduction lead to dissolution of enamel crystallites and caries formation (34); but this is an infectious disease, not an adaptation. Conversely, the same mechanism may be useful for enamel healing under different conditions.

The most sensible explanation for the porosity in enamel is that diffusion processes facilitate the self-healing of fractures. It is possible that the precipitation of organic and/or

mineral ions behind crack tips increases the strength and toughness of enamel, retarding crack propagation, as has been described for mica and silicate glass in aqueous solution (35). Conceivably, fractured enamel crystallite surfaces could seed mineral ions that diffuse through the enamel to bridge cracks. That calcium phosphate is supersaturated in saliva at neutral pH (36) is a rather significant piece of circumstantial evidence. However, remineralization phenomena are understood only from purely physicochemical kinetics and epidemiological studies involving fluoride supplementation. Caries research, while focused on topical fluoride-doped toothpastes and varnishes, has nevertheless demonstrated that it is only by frequent exposure to fluoride and incorporation of calcium fluorapatite into enamel that these studies and the ion transport through enamel pores can be explained (37). Ideally, though not necessarily through the same process as enamel self-healing, a bioceramic biomimetic design would ultimately be able to self-heal. This pursuit is an area of active research in the field of materials science and engineering, incorporating all classes of materials.

Aesthetics

Enamel is not normally brilliant white, in stark contrast to the monumental bleaching industry in dentistry fed by demands of people who want such teeth (38). Long wavelengths in the warm colors predominantly reflect from dentine, while shorter wavelengths in the blue range are contributed by enamel (39, 40). This, combined with a linear increase of light from enamel surface reflections in the visible spectrum, renders what is more or less a white or off-white tooth appearance. That light reflections from dentine contribute to tooth color is an indication that enamel efficiently transmits light through its substance, as has been documented (41). It is suggested that enamel crystallite surfaces are responsible for the short-wavelength reflections in enamel (40), but the crystal dimensions are so far below the wavelengths of the blue spectrum that this appears unlikely. However, enamel crystallite discontinuities do exist in the ca. 500-nm spatial domain, such as those in interpit enamel, which we suspect may be the source of the reflected light. Bioceramic biomimetic design of monolithic materials can accommodate the desire for whitish teeth by incorporating/generating a broad range of grain sizes, spanning 400–700 nm, to coincide with broad-spectrum reflections, with perhaps a greater emphasis on the shorter wavelengths for a brighter appearance.

Biofilm

Naturally occurring microscopic communities of bacteria live on wet enamel surfaces. Acidifying bacteria, such as *Streptococcus mutans*, if allowed to ascend the hierarchy of this

community, can lead to enamel dissolution and caries. For this reason, much attention has been paid to these "bad" bacteria, but one fascinating—and likely relevant—aspect to its presence is its exclusive maternal transmission (42, 43). More than a thousand resident gut bacteria have been identified to date; these are fundamental to human biological processes, from immunity to development, digestion, and metabolism, and, like *S. mutans*, are maternally acquired at birth (44). More than 700 species have been identified from the proximal end of the gastrointestinal tract, the oral cavity (45). As in any complex ecological community, some species will be freeloaders (commensal species), and others will consume our resources without providing anything back to us (parasitic species). But this ecological system has a long evolutionary history, and for all we know about the gut microbiome, many species in the oral cavity are likely working with our biology to contribute something to our survival (mutualist species).

Bioceramic biomimetic design should provide the nooks and crannies that nurture and protect oral biofilms. Human permanent teeth have a near-weekly incremental feature observed histologically, one that manifests on the surface as undulations or tile-like features called *perikymata,* which are visible to the naked eye (17). Perikymata are safe havens for bacteria; no existing toothbrush can reach into these crevices and valleys. A biomimetic surface design that provides the necessary residences required by our bacterial dwellers will be of some considerable benefit to them and to our well-being.

* * *

Although substantial advances have been made in ceramic engineering for dental restorations over the past decades, biomaterials scientists are still far from able to reproduce the three-dimensional functionally graded structures, mechanical properties, and aesthetic appearance of teeth. Nonetheless, advances both in materials and in fabrication methods have resulted in more durable and aesthetically pleasing ceramic restorative materials.

Mechanical Testing: Methods Currently Employed for Dental Ceramics

Alongside advances in materials and fabrication, mechanical testing methods for dental materials have evolved so as to be able to accelerate failures while mimicking clinically observed failure modes. Mechanical testing is used to ensure the treatment success of ceramic restorative materials, which depends on the effective transfer of cyclic stress through prosthetic components, tooth structures, and supporting tissues, such as the periodontal ligament and alveolar bone.

Although several studies utilize single-load-to-failure tests to obtain strength data, fatigue-testing methods have proven to be the most adequate and clinically relevant modalities for evaluating mechanical responses to dental ceramic systems. Fatigue is partially or totally related to failure, and the incidence of failure usually increases the longer the prosthetic components are loaded. Thus failure following fatigue is a time-dependent phenomenon.

There are a number of industrial devices available for repeatedly subjecting a specimen to controlled stress conditions during fatigue testing. However, because test accuracy depends on the simulation of real clinical conditions, some parameters should be controlled: cycling frequency, stress amplitude, dry–wet environment, temperature, and the reproduction of multidirectional functional loading, for example. The testing environment for novel ceramic restorative materials should comprise not only anatomically correct geometries but also a dynamic masticatory environment. Ideally, mechanical testing would be conducted in an accelerated fashion while providing clinically relevant fracture modes, thereby providing an informed platform for the further development of future ceramic restorative systems.

In the dental literature, several methods have commonly been used to test ceramic restorative materials under either static or dynamic conditions. Since modern testing techniques involve both setups, static and dynamic methods are both described below.

Single-Load-to-Failure Testing (Strength to Failure)

The *single-load-to-failure* (SLF) or *ultimate fracture strength* (UFS) test is characterized by loading of the specimen through compression until failure at a constant strain rate. During the test, a force–displacement curve is acquired for each specimen and the maximum load to failure is recorded.

Considering that this test approach involves loading the samples at stress levels higher than use stress in order to facilitate failures in a timely manner, *in vitro* studies have applied the technique to evaluate the strength of a multitude of prosthetic components. The classic limitation of single-load-to-failure methods relative to cyclic loading ones can be highlighted by comparing two studies from the same group of scientists. In the first study, Andriani et al. used the SLF mechanical testing setup to evaluate the strength to failure and fracture mode of three indirect composite materials directly applied onto titanium implant abutments and cemented porcelain-fused-to-metal crowns. In this study, specimens were loaded to failure in compression by applying a ramping force in the tip of one of the four cusps by means of an indenter at a rate of 1 mm/min in a universal testing machine (Instron 5666, Canton, MA). After failure, the fracture mode of the specimens was classified according to crack propagation direction. Overall,

Andriani et al.(46) concluded that no differences in strength existed among the materials, and that similar failure modes were observed between groups. Although from a mechanical and fractographic standpoint the study's methodology was sound, the strength to failure of all materials far exceeded physiologic loading conditions, resulting in fracture patterns not representative of clinical failures; this limited clinical insight on the further development of restorative materials. Such discrepancies between *in vitro* SLF results and clinically observed failures highlight what is known: in an oral environment, restorations are generally subjected not to increasing forces until failure, but rather to cumulative damage from high and low forces generated repeatedly during mastication.

In the follow-up study, Suzuki et al. (47) performed step-stress accelerated life testing (SSALT; described below) on the exact same specimen groups (and using the same physical configuration) as in the Andriani et al. (46) study, yet they obtained very different results. Crowns that had experienced a single-cycle load to failure exceeding 1000 N (strength to failure) presented a survival rate of only 40% when given a mission of 200,000 cycles at 200 N load (cumulative damage).

Fatigue

Fatigue is a mode of mechanical failure: Cracks are induced by subjecting a material or structure to repeated subcritical loads, which eventually leads to failure.[115] The term *fatigue* was first proposed by Jean-Victor Poncelet in 1839, a time when the Industrial Revolution had long been a reality and rapidly moving parts had become increasingly common. The main line of thought explained fatigue fractures by "crystallization" of the material, which became brittle after continued use and thus more prone to fracture.(48)

The fatigue resistance of a component is usually assessed by an *S–N* diagram, in which *S* is the stress and *N* is the number of cycles endured before failure. Most of the techniques suggested for this analysis are based on quantal data; that is, the number of "failures" or "survival" results at a given level of stress.

In dentistry, fatigue failure results from the development of microscopic cracks in areas of stress concentration that, under continued loading, fuse into an ever-growing fissure that weakens the restoration. (48) This initial step, termed *nucleation*, represents a mandatory stage of fatigue failure. When a fissure reaches its critical size, it will definitely progress at each loading cycle. This process, referred to as *propagation*, amounts to about 90% of fatigue life. At the end, *catastrophic failure* occurs as a result of a final loading cycle exceeding the mechanical capacity of the remaining sound portion of the material. (48)

Current research suggests that ceramic restorations failures are associated with damage accumulation generated by functional loading. Fatigue test methods have therefore become customary in dental materials testing laboratories, and variations among laboratories usually concern the fatigue method employed. There are presently three such methods often used for dental research: constant stress, staircase, and step-stress accelerated life testing. Regardless of the *in vitro* method used, any implant-supported prosthesis requires substantial evaluation before its release to clinical trials. Methods capable of predicting clinical performance over time are therefore highly desirable. Understanding the advantages and disadvantages of each of the three methods is necessary for critical evaluation of the current dental literature.

Constant Stress Test

A constant stress test is characterized by a material being cyclically tested under a constant load (Fig. 7). In order to simulate human masticatory function, several *in vitro* studies of dental materials exposed the specimens to constant stress.(49-54)
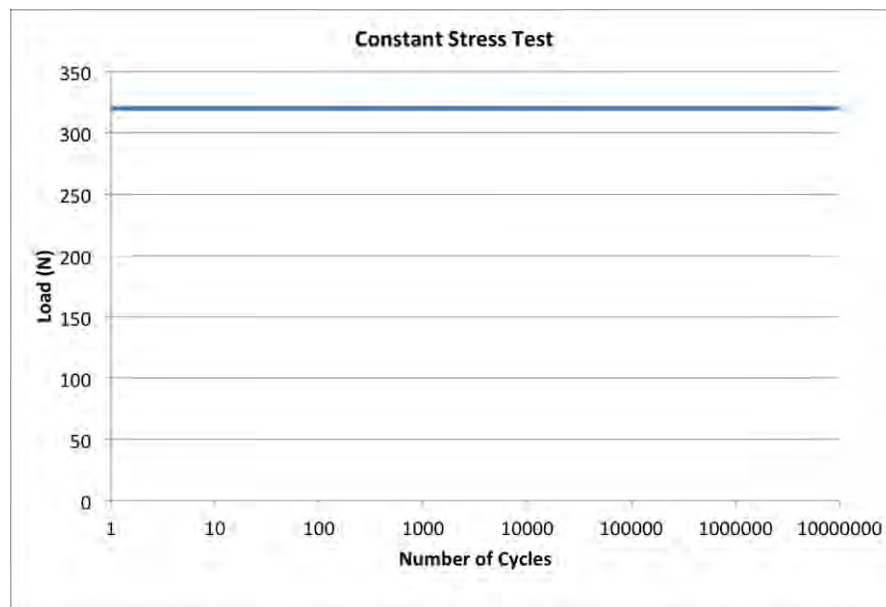

Figure 7. Example of a load of constant magnitude being applied over a number of cycles.

For instance, Assunção and coworkers (54) subjected single implant-supported prostheses to mechanical cycling with constant loads of 130 N in an attempt to simulate loading conditions in the anterior region of the mouth. Similarly, the dynamic fatigue properties of the

dental implant–abutment interface were simulated via constant stress by several other groups.(49-53)

According to the literature, (51, 54) an individual is assumed to present three episodes of chewing per day, each 15 min long, at a frequency of 60 cycles/min (1 Hz), resulting in 2700 cycles/day or almost 10^6 cycles during 1 year. However, to date, there is no consensus among *in vitro* study protocols regarding the number of test cycles in a constant stress test—it varies from 10^3 to 10^6 and up—making it difficult to compare results. Moreover, the frequency of load application, in hertz (cycles per second) has been reported to range from 2 Hz to 15 Hz. (53, 54) Thus, there is a need for further investigation concerning the parameters employed in this method and its correlation with clinical failures.

Staircase Method

The staircase method is a straightforward procedure in which a series of samples is tested sequentially to determine the median value of a fatigue limit. (55, 56) The test is conducted such that each specimen is tested for a determined lifetime corresponding to the infinite life. Although a life range of 10^6 to 10^8 cycles has been suggested, (55, 56) the number of cycles for which the component's fatigue strength will be determined can be guided by previous experience and based on the expected number of cycles to which the component is likely to be subjected during its intended life.

In the staircase method, if the specimen fails prior to infinite life, the next specimen will be tested at a lower stress level. If the specimen does not fail within this life of interest, the subsequent sample will be tested at a higher stress level. Therefore, specimens are tested one at a time, each test dependent on the previous result, with the stress level being increased or decreased by selected increments (1–2 standard deviations). It is recommended to run the test with at least 15–20 specimens (Fig. 8).(55-57)
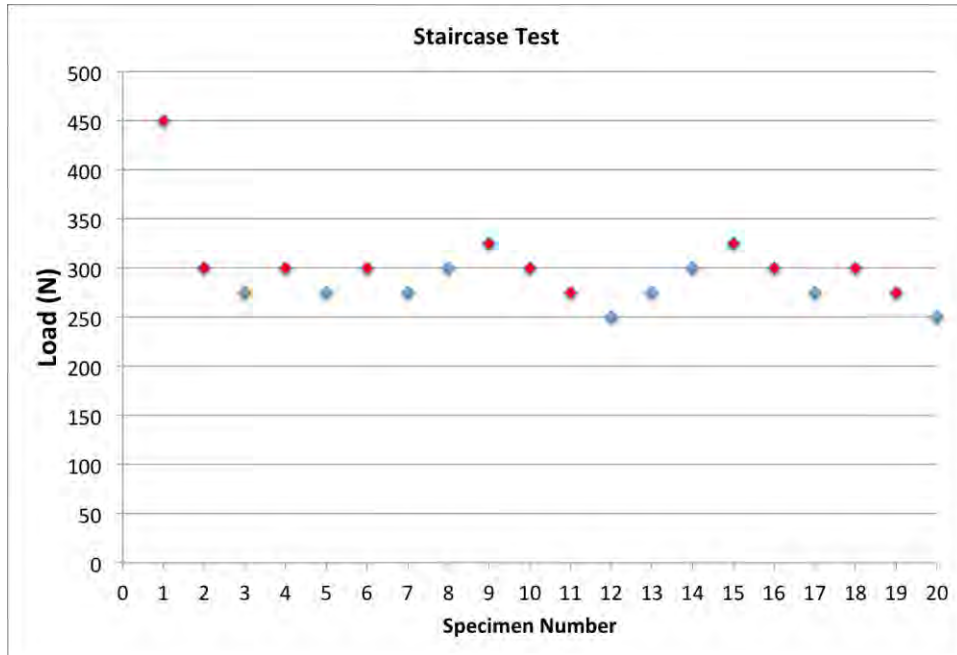
Figure 8. Representative staircase method test of 20 specimens subjected to constant fatigue until failure (red) or survival (blue) after a predetermined number of cycles. As shown, when a specimen fails, the next specimen is tested at a lower stress level; but if the specimen does not fail, the following test employs a higher stress level.

For example, Wiscott and coworkers (58) applied the staircase method to compare four abutment types to determine whether the connector's antirotational mechanism participates in fatigue resistance. The goal of the experiment was to determine the median fatigue strength—the stress level at which 50% of the specimens would survive 10^6 cycles and 50% would fail. In this study, the specimens were loaded to their long axis for a maximum of 10^6 cycles. Thereafter the test was halted, and the specimen was examined to determine whether it was broken or intact. If it had survived 10^6 cycles, the specimen was said to have "run out," and the next specimen was loaded to the previous magnitude plus 5 N. The same force (5 N) was subtracted from the former load magnitude if the previous specimen had failed. All told, 30 samples were tested in sequence.

Considering that median determination will properly begin only when the first turnaround (from lower to higher, or vice versa) occurs, extra samples may be necessary to set the initial stress amplitude for the procedure appropriately, (55, 57) which represents a cost increase for the experiment. However, an SLF test can previously be run as a pilot study to determine the entry stress level, thereby avoid fabrication of additional specimens for the staircase test.

At the end of the staircase testing sequence, data reduction techniques, such as the Dixon and Mood method or that or Zhang and Kececioglu, must be applied to determine the statistical distribution of the staircase test results.(55)

The Dixon and Mood method is based on the maximum likelihood estimation (MLE) and calculates the mean and standard deviation of a fatigue limit that follows a normal distribution. This approach considers either only the failures or only the survivals to determine the statistical properties and is dependent on the least frequent event. The method was proposed at a time when computing power was a scarce resource and simple, approximate methods were correspondingly valuable. (57) On the other hand, the Zhang and Kececioglu method considers the suspended items (i.e., those removed from the test prior to failure) and the MLE for the data. It is usually applied if the Dixon and Mood method is not indicated; that is, when the fatigue limit is not normal, the stress increments are not identical, and the stress increment is greater than twice the standard deviation. (55)

Although the staircase method is an easy, "up and down" sequential technique for estimating the fatigue strength of a component or material, its accuracy and many sensitivity factors may be questioned. For instance, the test is not conducted in a wide force range, and the sample is not submitted to extreme stress values, which could mask the maximum strength of the material. In addition, the number of cycles to determine the failure or survival of each specimen is predetermined, avoiding the simulation of material performance for a longer period.

Step-Stress Accelerated Life Testing

Step-stress accelerated life testing (SSALT) is a mechanical (fatigue) test method for shortening the life of materials or hastening the degradation of their performance. It is intended to obtain quickly data that, properly modeled and analyzed, yield desired information on product life or performance under normal use. (59) The SSALT method allows the prediction with confidence intervals (based on calculation of a master Weibull distribution) of the life expectancy of a given material under specified loading. (Computer software is available for life expectancy calculations)

In SSALT, a specimen is subjected to successively higher levels of stress. First, each specimen is submitted to constant stress during a predetermined length of time. The stress on this specimen is then increased step by step until its failure or survival. SSALT has been widely applied for metals, plastics, dielectrics and insulations, ceramics, rubber and elastics, food and drugs, lubricants, protective coating and paints, concrete and cement, building materials, and nuclear reactor materials. A similar process has also been implemented for biomaterials used in

dentistry, such as ceramic restorations, dental implants, and adhesive bond material. (47, 60-84)

Previous work (47, 60-84) using SSALT in dentistry has utilized SLF as the first step to determine step-stress accelerated life-testing profiles (usually three: mild, moderate, and aggressive) (Fig. 9). The use of at least three profiles for this type of testing reflects the need to distribute failure across different step loads and allows better prediction statistics, narrowing confidence intervals. Mild, moderate, and aggressive refer to the increasingly stepwise rapidity with which a specimen is fatigued to reach a certain level of load; that is, specimens assigned to a mild profile will be cycled longer to reach the same load of a specimen assigned to either a moderate or aggressive profile. These profiles usually begin at a load that is approximately 30% of the mean value of SLF and end at a load roughly 60% of the same value.
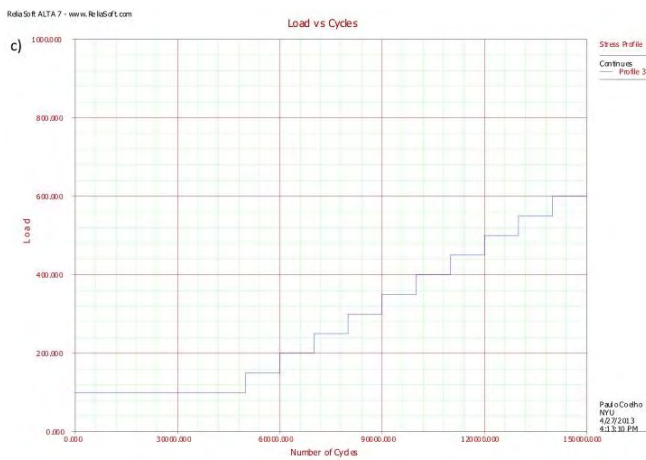
Several previous investigations (47, 60-84) have demonstrated that 18 specimens are usually enough to obtain good linear regression fits. Previous work in the dental literature has thus used 3 specimens subjected to initial SLF and 18 then assigned to mild (n = 9), moderate (n = 6), and aggressive (n = 3) fatigue profiles—a ratio of 3:2:1 (although 4:2:1 has also been used) (Fig. 9).

(a)
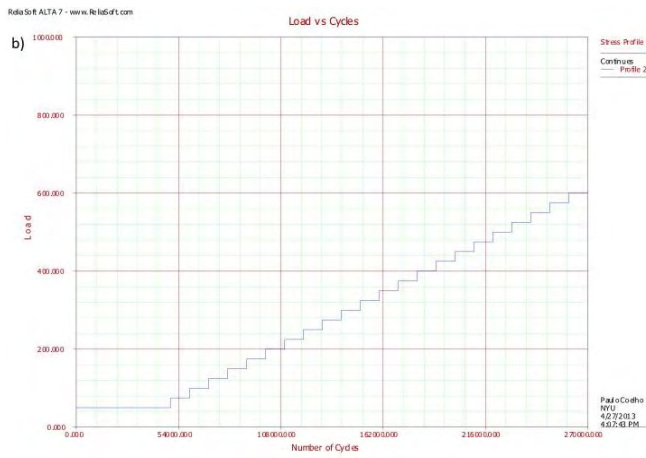
(b)

(c)

Figure 9. Charts illustrating the step-stress (a) mild, (b) moderate, and (c) aggressive profiles used for an accelerated fatigue test. Note that an increase overall slope (i.e., load/number of cycles) occurs from mild to moderate, and from moderate to aggressive profiles.

Following the parameters of loading for each predetermined profile, the specimens are fatigued until failure or survival (no failure at the end of step-stress profiles), where maximum loads are applied up to a limit previously established based on SLF mean value (N).

Based upon the step-stress distribution of the failures, the fatigue data are analyzed using a power law relationship for damage accumulation and the use level probability Weibull curves (probability of failure vs. cycles) at a use stress load are determined for life expectancy calculations by using a specific software (Alta Pro 7, Reliasoft, Tucson, AZ). The use level probability Weibull analysis provides a beta (β) value, which describes the failure rate behavior over time. (β < 1: failure rate decreases over time, commonly associated with "early failures" or failures that occur due to egregious flaws; β ~ 1: failure rate does not vary over time, associated with failures of a random nature; β > 1: failure rate increases over time, associated with failures related to damage accumulation.) A reliability calculation (with two-sided confidence bounds that can be calculated by a variety of methods, including the MLE) is then mathematically estimated for the completion of a given number of cycles (mission) at a specific load level (Fig. 10).

If when testing, say, crown–implant systems, the use level probability Weibull–calculated beta (β) is <1 for any tested group, then the crown–implant system failure is primarily driven by system strength rather than damage accumulation from fatigue testing. In that case, a Weibull two-parameter can be calculated (Weibull 7++, Reliasoft, Tucson, AZ) using only the final load at failure or survival of specimens (i.e., disregarding the number of cycles) (Fig. 11). (47, 60-85)

A\A: Beta= 3.2915; Alpha(0)=15.5719; Alpha(1)=-0.8796
B\B: Beta=0.5901; Alpha(0)=53.3662; Alpha(1)=-8.2757
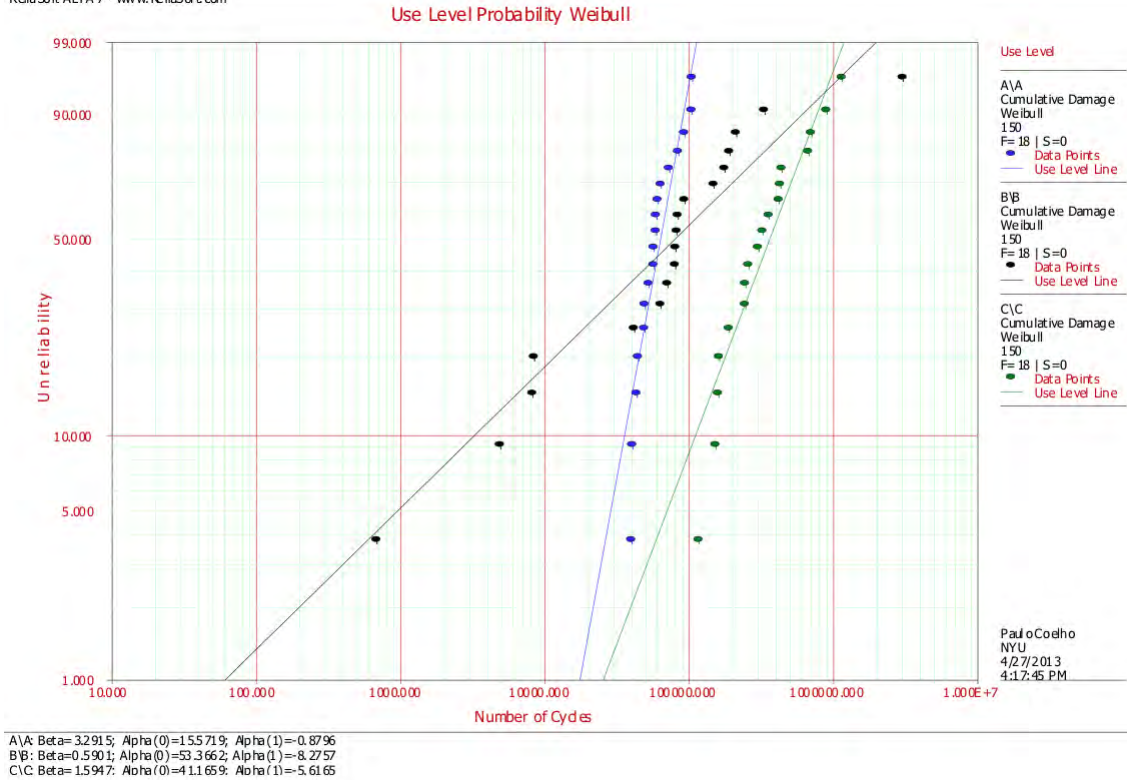C\C: Beta= 1.5947: Alpha(0)=41.1659: Alpha(1)=-5.6165

Figure 10. Theoretical use level probability calculation for materials A, B, and C, where the probability of failure was calculated for a 150-N use load. Note the different degrees of linear fit and the differences in beta (β) values for the three different materials.

An instructive graphical method to determine whether these data sets are significantly different (based upon nonoverlap of confidence bounds) is the utilization of a Weibull 2-parameter contour plot (Weibull modulus m vs. characteristic strength η [eta] (Fig. 11). Weibull modulus m is an indicator of strength reliability and/or the asymmetrical strength distribution as a result of flaws within the material. It is often used in evaluating ceramics and other brittle materials. A higher m indicates smaller and/or fewer defects (greater structural reliability); a lower m is evidence of greater variability of the strength, reflecting more flaws in the system and a decrease in reliability (85).

Contour Plot

Contour

A\A
Weibull-2P
RRX SRM MED FM
F=17/S=0
—— 90%

B\B
Weibull-2P
RRX SRM MED FM
F=18/S=0
—— 90%

C\C
Weibull-2P
RRX SRM MED FM
F=18/S=0
—— 90%

E

20.000

16.400

12.800

9.200

5.600

2.000

0.000   100.000   200.000   300.000   400.000   500.000

Eta

PauloCoelho
NYU
4/27/2013
4:22:25 PM

A\A: β=9.6765, η=173.4897, ρ=0.9439
B\B: β=10.6501, η=256.9513, ρ=0.9267
C\C: β=8.2105, η=360.9641, ρ=0.9337

Figure 11. Theoretical Weibull parameter contour plot (Weibull modulus *m* vs. characteristic strength η [eta]) for materials A, B, and C. The bounded areas represent all potential combinations of characteristic strength (η, which indicates the load at which 63.2% of the specimens of each group fail) and Weibull modulus (*m,* based on Weibull load to failure distribution) at a 95% level of confidence. In summary, materials that present themselves to the right and to the top of the graph are stronger and present a narrower load to failure distribution, respectively.

In dentistry, especially for dental ceramics testing, the SSALT method can be employed using a servo-all-electric system, where the indenter contacts the specimen surface, applies the prescribed load within the step profile, and lifts off of the material surface. However, the step-stress method can also be conducted with an electrodynamic testing machine to simulate mouth-motion fatigue (MMSSALT). (65, 68, 79-81) Thus, specimens can be tested in either axial or off-axis loading orientation. (47, 60-85)

The applicability of SSALT in the evaluation of dental ceramics has been demonstrated by a series of studies using different ceramic materials and geometric configurations (65, 68, 79-81). Of special interest is that, for this series of studies, all specimens presented standardized geometric configurations and thus may be compared with one another. In addition, dental ceramics testing performed by MMSSALT has thus far been shown to be the only testing method able to reproduce *in vitro* the fracture modes observed clinically (65, 68, 79-81). This

provides dental ceramics developers with an informed platform, one that is currently being utilized to improve dental ceramic systems for the future.

The main advantage of a step-stress test is that it quickly yields failures; the increasing stress levels ensure this. However, quick failures do not guarantee more accurate estimates. A constant fatigue test with a few specimen failures usually yields greater accuracy than a shorter step-stress test in which all specimens fail; it is the total time on test (summed over all specimens), not the number of failures, that determines accuracy. (59) One disadvantage of step-stress tests is that under clinical conditions most specimens run at constant stress, not step stress. Thus, the tested model must properly take into account the cumulative effect of exposure at successive stresses. Moreover, the model must also provide an estimate of life under constant stress that should not exceed 3–4 times the average number of cycles employed throughout the test for all groups. (59)

Conclusions

We conclude that there are several attributes of enamel that are of relevance to biomimetic bioceramic design. While it may not be required to adopt the same microstructure, it may be of some importance to manufacture discontinuites in all 360° spherical rotational positions at hierarchies of scale from nano- to micro-levels. It may also be useful to design a sensing technology that elicits a neuromusculature response to overloading. Further, because even nanoscopic fractures have the capacity to grow, bioceramic compositions should be developed that favor calcium carbonitic annealing over the usual propensities for these cracks to be filled with organics. Aesthetics will always be a major concern in bioceramic design, however this should not obviate the need to maintain surface structures that protect the oral biota; we have no knowledge about whether this has any relevance to human health at present, but until such time that we do, it may be wise to side with nature.

A number of mechanical testing methods have been reviewed, but above all, whichever method has merit for a particular study, it is important that the cycling frequency, stress amplitude, dry–wet environment (the latter preferred), temperature, and the reproduction of multidirectional functional loading are controlled for in the experiment. Further, attention to anatomically correct geometries and dynamic masticatory environments will bear more relevance to *in vivo* conditions. In an oral environment, cumulative damage is the result of high and low forces generated repeatedly during mastication, leading to the development of microscopic cracks in areas of stress concentration and fatigue failure. While we are unaware of studies on the statistical distribution of forces, we suspect that over reasonable time frames

(e.g., one week to a month), this distribution has structure and obeys a power law. In this respect, we highlight step-stress accelerated life testing as a method that, while experimentally relatively fast, may have more relevance to the determination of life expectancy calculations and to the reproduction of *in vitro* fracture modes observed clinically than other methods.

Acknowledgments

References

1.	Chadwick DJ, Cardew G. Dental Enamel. West Sussex: John Wiley & Sons Ltd.; 1997.

2.	Lacruz RS, Smith CE, Moffatt P, Chang EH, Bromage TG, Bringas PJ, et al. Requirements for Ion and Solute Transport, and pH Regulation During Enamel Maturation. Journal of Cellular Physiology. 2012;227:1776-85.

3.	Benazzi S, Kullmer O, Grosse IR, Weber GW. Using occlusal wear information and finite element analysis to investigate stress distributions in human molars. Journal of Anatomy. 2011;219:259–72.

4.	Benazzi S, Kullmer O, Grosse IR, Weber GW. Comparing Loading Scenarios in Lower First Molar Supporting Bone Structure Using 3D Finite Element Analysis. American Journal of Physical Anthropology. 2012;147:128–34.

5.	Kono RT, G.Suwa, T.Tanijiri. A three-dimensional analysis of enamel distribution patterns in human permanent first molars. Archives of Oral Biology. 2002 47:867-75.

6.	Vogel ER, Woerden JTv, Lucas PW, Atmoko SSU, Schaik CPv, Dominy NJ. Functional ecology and evolution of hominoid molar enamel thickness- Pan troglodytes schweinfurthii and Pongo pygmaeus wurmbii. Journal of Human Evolution. 2008;55:60-74.

7.	Cuy JL, Mann AB, Livi KJ, Teaford MF, Weihs TP. Nanoindentation mapping of the mechanical properties of human molar tooth enamel. Archives of Oral Biology. 2002;47:281-91.

8.	Marshall GWJ, Balooch M, Gallagher RR, Gansky SA, Marshall SJ. Mechanical properties of the dentoenamel junction: AFM studies of nanohardness, elastic modulus, and fracture. Journal of Biomedical Materials Research. 2001;54:87-95.

9.	Imbeni V, Kruzic JJ, Marshall GW, Marshall SJ, Ritchie RO. The dentin-enamel junction and the fracture of human teeth. Nature Materials. 2005;4:229-32.

10.	Zaslansky P, Friesem AA, Weiner S. Structure and mechanical properties of the soft zone separating bulk dentin and enamel in crowns of human teeth: Insight into tooth function. Journal of Structural Biology. 2006;153 188-99.

11.	Lynch CD, O'Sullivan VR, Dockery P, McGillycuddy CT, Sloan AJ. Hunter-Schreger Band patterns in human tooth enamel. Journal of Anatomy. 2010;217:106-15.

12.	Hanaizumi Y, Maeda T, Takano T. Three-dimensional arrangement of enamel prisms and their relationship to the formation of Hunter-Schreger bands in dog tooth. Cell and Tissue Research. 1996;286:103-14.

13.	Bajaj D, Arola D. Role of Prism Decussation on Fatigue Crack Growth and Fracture of Human Enamel. Acta Biomaterialia. 2009;5:3045–56.

14.	Chai H, Lee JJ-W, Constantino PJ, Lucas PW, Lawn BR. Remarkable resilience of teeth. Proceedings of the National Academy of Sciences. 2009;106:7289–93.

15.	Lucas P, Constantino P, Wood B, Lawn B. Dental enamel as a dietary indicator in mammals. BioEssays. 2008;30:374-85.

16.	Boyde A. Enamel. In: Oksche A, Vollrath L, editors. Handbook of Microscopic Anatomy. Berlin: Springer Verlag; 1989. p. 309-473.

17.	Boyde A. Microstructure of enamel. In: Chadwick DJ, Cardew G, editors. Dental Enamel. West Sussex: John Wiley & Sons Ltd.; 1997. p. 18-31.

18.	Lacruz RS, Hacia JG, Bromage TG, Boyde A, Lei Y, Xu Y, et al. The Circadian Clock Modulates Enamel Development. Journal of Biological Rhythms. 2012;27:237-45.

19.	Boyde A. Enamel structure and cavity margins. Operative Dentistry. 1976;1:13-28.

20.	Gao H, Ji B, Jaëger IL, Arzt E, Fratzl P. Materials become insensitive to flaws at nanoscale: Lessons from nature. Proceedings of the National Academy of Sciences. 2003;100:5597–600.

21.	He LH, Swain MV. Understanding the mechanical behaviour of human enamel from its structural and compositional characteristics. Journal of the Mechanical Behavior of Biomedical Materials. 2008;1:18-29.

22.   Smith BL, Schäffer TE, Viani M, Thompson JB, Frederick NA, Kindt J, et al. Molecular mechanistic origin of the toughness of natural adhesives, fibres and composites. Nature Materials. 1999 399:761-3.

23.   Dibdin GH. The Stability of Water in Human Dental Enamel Studied by Proton Nuclear Magnetic Resonance. Archives of Oral Biology. 1972;17:433-7.

24.   Zahradnik RT, Moreno EC. Structural features of human dental enamel as revealed by isothermal water vapour sorption. Archives of Oral Biology. 1975;20:317-25.

25.   Nyman JS, Ni Q, Nicolella DP, Wang X. Measurements of mobile and bound water by nuclear magnetic resonance correlate with mechanical properties of bone. Bone. 2008;42:193–9.

26.   Stanford JW, Weigel KV, Paffenbarger GC, Sweeney WT. Compressive properties of hard tooth tissues and some restorative materials. Journal of the American Dental Association. 1960;60:746-56.

27.   Boyde A. Dependence of rate of physical erosion on orientation and density in mineralized tissues. Anatomy and embryology. 1984;170:57-62.

28.   Shimizu D, Macho GA. Effect of Enamel Prism Decussation and Chemical Composition on the Biomechanical Behavior of Dental Tissue: A Theoretical Approach to Determine the Loading Conditions to Which Modern Human Teeth Are Adapted. The Anatomical Record. 2008;291:175-82.

29.   Macho GA, Shimizu D. Kinematic parameters inferred from enamel microstructure: new insights into the diet of Australopithecus anamensis. Journal of Human Evolution. 2010;58:23-32.

30.   Grieznis L, Apse P, Blumfelds L. Passive tactile sensibility of teeth and osseointegrated dental implants in the maxilla. Stomatologija, Baltic Dental and maxillofacial Journal. 2010;12:80-6.

31.   Dibdin GH. The water in human dental enamel and its diffusional exchange measdured by clearance of tritiated water from enamel slabs of varying thickness. Caries Research. 1993;27:81-6.

32.   Flim GJ, Arends J. The Temperature Dependency of 45Ca Diffusion in Bovine Enamel. Calcified Tissue Research. 1977;24:173-7.

33.   Rooij JFd, Arends J. Phosphate diffusion in whole bovine enamel. Caries Research. 1982;16:211-6.

34.   Shellis RP, Dibdin GH. Enamel microporosity and its functional implications. In: Teaford MF, Smith MM, Ferguson MWJ, editors. Development, Function and Evolution of Teeth. Cambridge: Cambridge University Press; 2000. p. 242-51.

35.   Roach DH, Lathabai S, Lawn BR. Interfacial layers in brittle cracks. Journal of the American Ceramic Society. 1988;71:97-105.

36.   Hicks J, Flaitz C. Role of remineralizing fluid in in vitro enamel caries formation and progression. Quintessence International. 2007;38:313-9.

37.   Cate JMt, Feathestone JDB. Physicochemical aspects of fluoride-enamel interactions. In: Fejerskov O, Eksrand J, Burt BA, editors. Fluoride in Dentistry. 2nd ed. Copenhagen: Munksgaard; 1996. p. 252-72.

38.   Greenwall L, editor. Bleaching Techniques in Restorative Dentistry: An Illustrated Guide. London: Martin Dunitz; 2001.

39.   Bosch JJt, Coops JC. Tooth color and reflectance as related to light scattering and enamel hardness. Journal of Dental Research. 1995;74:374-80.

40.   Vaarkamp J, Bosch JJt, Verdonschot EH. Propagation of light through human dental enamel and dentine. Caries Research. 1995;29:8-13.

41.   Odor TM, Watson TF, Ford TRP, Mcdonald F. Pattern of transmission of laser light in teeth. International Endodontic Journal. 1996;29:228-34.

42. Li Y, Caufield PW. The fidelity of initial acquisition of mutans streptococci by infants from their mothers. Journal of Dental Research. 1995;74:681-5.

43. Li Y, Dasanayake AP, Caufield PW, Elliott RR, Butts JT. Characterization of maternal mutans streptococci transmission in an African American population. The Dental Clinics of North America. 2003;47:87-101.

44. Nicholson JK, Holmes E, I.D.Wilson. Gut microorganisms, mammalian metabolism and personalized health care. Nature Reviews Microbiology. 2005;3:431-8.

45. Zijnge V, Leeuwen MBMv, Degener JE, Abbas F, Thurnheer T, Gmür R, et al. Oral Biofilm Architecture on Natural Teeth. PLoS one. 2010;5(2):e9231

46. Andriani W, Jr., Suzuki M, Bonfante EA, Carvalho RM, Silva NR, Coelho PG. Mechanical testing of indirect composite materials directly applied on implant abutments. The journal of adhesive dentistry. 2010;12(4):311-7. doi: 10.3290/j.jad.a17710. PubMed PMID: 20157657.

47. Suzuki M, Bonfante E, Silva NR, Coelho PG. Reliability testing of indirect composites as single implant restorations. Journal of prosthodontics : official journal of the American College of Prosthodontists. 2011;20(7):528-34. doi: 10.1111/j.1532-849X.2011.00754.x. PubMed PMID: 22003830.

48. Wiskott HW, Nicholls JI, Belser UC. Stress fatigue: basic principles and prosthodontic implications. The International journal of prosthodontics. 1995;8(2):105-16. PubMed PMID: 7575960.

49. Quek HC, Tan KB, Nicholls JI. Load fatigue performance of four implant-abutment interface designs: effect of torque level and implant system. The International journal of oral & maxillofacial implants. 2008;23(2):253-62. PubMed PMID: 18548921.

50. Hoyer SA, Stanford CM, Buranadham S, Fridrich T, Wagner J, Gratton D. Dynamic fatigue properties of the dental implant-abutment interface: joint opening in wide-diameter versus standard-diameter hex-type implants. The Journal of prosthetic dentistry. 2001;85(6):599-607. doi: 10.1067/mpr.2001.115250. PubMed PMID: 11404760.

51. Gratton DG, Aquilino SA, Stanford CM. Micromotion and dynamic fatigue properties of the dental implant-abutment interface. The Journal of prosthetic dentistry. 2001;85(1):47-52. doi: 10.1067/mpr.2001.112796. PubMed PMID: 11174678.

52. Cibirka RM, Nelson SK, Lang BR, Rueggeberg FA. Examination of the implant-abutment interface after fatigue testing. The Journal of prosthetic dentistry. 2001;85(3):268-75. doi: 10.1067/mpr.2001.114266. PubMed PMID: 11264934.

53. Boggan RS, Strong JT, Misch CE, Bidez MW. Influence of hex geometry and prosthetic table width on static and fatigue strength of dental implants. The Journal of prosthetic dentistry. 1999;82(4):436-40. PubMed PMID: 10512962.

54. Assuncao WG, Barao VA, Delben JA, Gomes EA, Garcia IR, Jr. Effect of unilateral misfit on preload of retention screws of implant-supported prostheses submitted to mechanical cycling. Journal of prosthodontic research. 2011;55(1):12-8. doi: 10.1016/j.jpor.2010.05.002. PubMed PMID: 20627771.

55. SK L, YL L, MW L. Evaluation of the staircase and the accelerated methods for fatigue limit distributions. International Journal of Fatigue

. 2001;23:75-83.

56. J S, ZP M, RJ G, PN. C. Sensitivity study of staircase fatigue tests using Monte Carlo simulation. . SAE. 2005.

57. Grove D CF. A comparison of two methods of analysing staircase fatigue test data. . Quality and Reliability Engineering International 2008;24:485-97.

58. Wiskott HW, Jaquet R, Scherrer SS, Belser UC. Resistance of internal-connection implant connectors under rotational fatigue loading. The International journal of oral & maxillofacial implants. 2007;22(2):249-57. PubMed PMID: 17465350.

59.   Nelson W. Accelerated Testing: Statistical Models, Test Plans, and Data Analysis. . Wiley. 1990;New York.

60.   Almeida EO, Freitas AC, Jr., Bonfante EA, Marotta L, Silva NR, Coelho PG. Mechanical testing of implant-supported anterior crowns with different implant/abutment connections. The International journal of oral & maxillofacial implants. 2013;28(1):103-8. doi: 10.11607/jomi.2443. PubMed PMID: 23377054.

61.   Almeida EO, Freitas Junior AC, Bonfante EA, Rocha EP, Silva NR, Coelho PG. Effect of microthread presence and restoration design (screw versus cemented) in dental implant reliability and failure modes. Clinical oral implants research. 2013;24(2):191-6. doi: 10.1111/j.1600-0501.2012.02437.x. PubMed PMID: 22413873.

62.   Almeida EO, Junior AC, Bonfante EA, Silva NR, Coelho PG. Reliability evaluation of alumina-blasted/acid-etched versus laser-sintered dental implants. Lasers in medical science. 2013;28(3):851-8. doi: 10.1007/s10103-012-1170-8. PubMed PMID: 22843309.

63.   Bonfante EA, Coelho PG, Guess PC, Thompson VP, Silva NR. Fatigue and damage accumulation of veneer porcelain pressed on Y-TZP. Journal of dentistry. 2010;38(4):318-24. doi: 10.1016/j.jdent.2009.12.004. PubMed PMID: 20026232.

64.   Bonfante EA, Coelho PG, Navarro JM, Jr., Pegoraro LF, Bonfante G, Thompson VP, et al. Reliability and failure modes of implant-supported Y-TZP and MCR three-unit bridges. Clinical implant dentistry and related research. 2010;12(3):235-43. doi: 10.1111/j.1708-8208.2009.00156.x. PubMed PMID: 19416277.

65.   Bonfante EA, Rafferty B, Zavanelli RA, Silva NR, Rekow ED, Thompson VP, et al. Thermal/mechanical simulation and laboratory fatigue testing of an alternative yttria tetragonal zirconia polycrystal core-veneer all-ceramic layered crown design. European journal of oral sciences. 2010;118(2):202-9. doi: 10.1111/j.1600-0722.2010.00724.x. PubMed PMID: 20487011.

66.   Bonfante EA, Sailer I, Silva NR, Thompson VP, Dianne Rekow E, Coelho PG. Failure modes of Y-TZP crowns at different cusp inclines. Journal of dentistry. 2010;38(9):707-12. doi: 10.1016/j.jdent.2010.04.001. PubMed PMID: 20382197.

67.   Bonfante EA, Suzuki M, Lubelski W, Thompson VP, de Carvalho RM, Witek L, et al. Abutment design for implant-supported indirect composite molar crowns: reliability and fractography. Journal of prosthodontics : official journal of the American College of Prosthodontists. 2012;21(8):596-603. doi: 10.1111/j.1532-849X.2012.00872.x. PubMed PMID: 22672650.

68.   Coelho PG, Silva NR, Bonfante EA, Guess PC, Rekow ED, Thompson VP. Fatigue testing of two porcelain-zirconia all-ceramic crown systems. Dental materials : official publication of the Academy of Dental Materials. 2009;25(9):1122-7. doi: 10.1016/j.dental.2009.03.009. PubMed PMID: 19395078.

69.   Freitas AC, Jr., Bonfante EA, Martins LM, Silva NR, Marotta L, Coelho PG. Reliability and failure modes of anterior single-unit implant-supported restorations. Clinical oral implants research. 2012;23(9):1005-11. doi: 10.1111/j.1600-0501.2011.02269.x. PubMed PMID: 22092676.

70.   Freitas AC, Jr., Bonfante EA, Rocha EP, Silva NR, Marotta L, Coelho PG. Effect of implant connection and restoration design (screwed vs. cemented) in reliability and failure modes of anterior crowns. European journal of oral sciences. 2011;119(4):323-30. doi: 10.1111/j.1600-0722.2011.00837.x. PubMed PMID: 21726295.

71.   Freitas Junior AC, Bonfante EA, Silva NR, Marotta L, Coelho PG. Effect of implant-abutment connection design on reliability of crowns: regular vs. horizontal mismatched platform. Clinical oral implants research. 2012;23(9):1123-6. doi: 10.1111/j.1600-0501.2011.02257.x. PubMed PMID: 22092300.

72.   Freitas-Junior AC, Almeida EO, Bonfante EA, Silva NR, Coelho PG. Reliability and failure modes of internal conical dental implant connections. Clinical oral implants research. 2013;24(2):197-202. doi: 10.1111/j.1600-0501.2012.02443.x. PubMed PMID: 22429387.

73.   Freitas-Junior AC, Bonfante EA, Martins LM, Silva NR, Marotta L, Coelho PG. Effect of implant diameter on reliability and failure modes of molar crowns. The International journal of prosthodontics. 2011;24(6):557-61. PubMed PMID: 22146255.

74.   Freitas-Junior AC, Rocha EP, Bonfante EA, Almeida EO, Anchieta RB, Martini AP, et al. Biomechanical evaluation of internal and external hexagon platform switched implant-abutment connections: An in vitro laboratory and three-dimensional finite element analysis. Dental materials : official publication of the Academy of Dental Materials. 2012;28(10):e218-28. doi: 10.1016/j.dental.2012.05.004. PubMed PMID: 22682782.

75.   Guess PC, Bonfante EA, Silva NR, Coelho PG, Thompson VP. Effect of core design and veneering technique on damage and reliability of Y-TZP-supported crowns. Dental materials : official publication of the Academy of Dental Materials. 2013;29(3):307-16. doi: 10.1016/j.dental.2012.11.012. PubMed PMID: 23228337.

76.   Guess PC, Zavanelli RA, Silva NR, Bonfante EA, Coelho PG, Thompson VP. Monolithic CAD/CAM lithium disilicate versus veneered Y-TZP crowns: comparison of failure modes and reliability after fatigue. The International journal of prosthodontics. 2010;23(5):434-42. PubMed PMID: 20859559.

77.   Martins LM, Bonfante EA, Zavanelli RA, Freitas AC, Jr., Silva NR, Marotta L, et al. Fatigue reliability of 3 single-unit implant-abutment designs. Implant dentistry. 2012;21(1):67-71. doi: 10.1097/ID.0b013e31823fcc9f. PubMed PMID: 22228459.

78.   Sanon C, Chevalier J, Douillard T, Kohal RJ, Coelho PG, Hjerppe J, et al. Low temperature degradation and reliability of one-piece ceramic oral implants with a porous surface. Dental materials : official publication of the Academy of Dental Materials. 2013;29(4):389-97. doi: 10.1016/j.dental.2013.01.007. PubMed PMID: 23419633.

79.   Silva NR, Bonfante EA, Martins LM, Valverde GB, Thompson VP, Ferencz JL, et al. Reliability of reduced-thickness and thinly veneered lithium disilicate crowns. Journal of dental research. 2012;91(3):305-10. doi: 10.1177/0022034511433504. PubMed PMID: 22205635; PubMed Central PMCID: PMC3275335.

80.   Silva NR, Bonfante EA, Rafferty BT, Zavanelli RA, Rekow ED, Thompson VP, et al. Modified Y-TZP core design improves all-ceramic crown reliability. Journal of dental research. 2011;90(1):104-8. doi: 10.1177/0022034510384617. PubMed PMID: 21057036; PubMed Central PMCID: PMC3144096.

81.   Silva NR, Bonfante EA, Zavanelli RA, Thompson VP, Ferencz JL, Coelho PG. Reliability of metalloceramic and zirconia-based ceramic crowns. Journal of dental research. 2010;89(10):1051-6. doi: 10.1177/0022034510375826. PubMed PMID: 20660796; PubMed Central PMCID: PMC3318053.

82.   Silva NR, Coelho PG, Fernandes CA, Navarro JM, Dias RA, Thompson VP. Reliability of one-piece ceramic implant. Journal of biomedical materials research Part B, Applied biomaterials. 2009;88(2):419-26. doi: 10.1002/jbm.b.31113. PubMed PMID: 18491412.

83.   Silva NR, de Souza GM, Coelho PG, Stappert CF, Clark EA, Rekow ED, et al. Effect of water storage time and composite cement thickness on fatigue of a glass-ceramic trilayer system. Journal of biomedical materials research Part B, Applied biomaterials. 2008;84(1):117-23. doi: 10.1002/jbm.b.30851. PubMed PMID: 17455281.

84.   Silva NR, Thompson VP, Valverde GB, Coelho PG, Powers JM, Farah JW, et al. Comparative reliability analyses of zirconium oxide and lithium disilicate restorations in vitro and in vivo. Journal of the American Dental Association. 2011;142 Suppl 2:4S-9S. PubMed PMID: 21454834.

85.   Ritter JE. Predicting lifetimes of materials and material structures. Dental materials : official publication of the Academy of Dental Materials. 1995;11(2):142-6. doi: 10.1016/0109-5641(95)80050-6. PubMed PMID: 8621036.